JACS
JOURNAL OF THE AMERICAN CHEMICAL SOCIETY
Article
pubs.acs.org/JACS

Structural Factors Controlling the Spin–Spin Exchange Coupling: EPR Spectroscopic Studies of Highly Asymmetric Trityl–Nitroxide Biradicals

Yangping Liu,[†] Frederick A. Villamena,[†,‡] Antal Rockenbauer,*[,§] Yuguang Song,[†] and Jay L. Zweier*[,†]

[†]Center for Biomedical EPR Spectroscopy and Imaging, The Davis Heart and Lung Research Institute, Division of Cardiovascular Medicine, Department of Internal Medicine, and [‡]Department of Pharmacology, College of Medicine, The Ohio State University, Columbus, Ohio 43210, United States

[§]Institute of Molecular Pharmacology, Research Centre for Natural Sciences, Hungarian Academy of Sciences, P.O. Box 17, H-1525 Budapest, Hungary

Supporting Information

ABSTRACT: Highly asymmetric exchange-coupled biradicals, e.g., the trityl–nitroxides (TNs), possess particular magnetic properties that have opened new possibilities for their application in biophysical, physicochemical, and biological studies. In the present work, we investigated the effect of the linker length on the spin–spin coupling interaction (J) in TN biradicals using the newly synthesized biradicals CT02-GT, CT02-AT, CT02-VT, and CT02-PPT as well as the previously reported biradicals TNN14 and TN1. The results show that the magnitude of J can be easily tuned from ~4 G (conformer 1 in CT02-PPT) to >1200 G (in TNN14) by varying the linker separating the two radical moieties and changing the temperature. Computer simulations of EPR spectra were carried out to estimate J values of the TN biradicals directly. In addition to the spin–spin coupling interaction of TN biradicals, their g, hyperfine-splitting, and zero-field-splitting interactions were explored at low temperature (220 K). Our present study clearly shows that varying the spin–spin interaction as a function of linker distance and temperature provides an effective strategy for the development of new TN biradicals that can find wide applications in relevant fields.

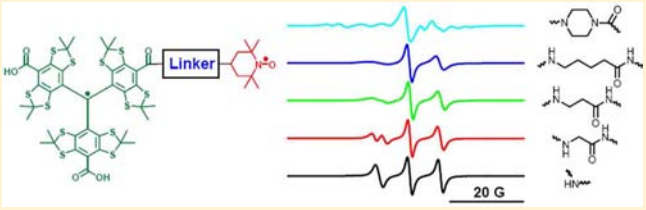

INTRODUCTION

Exchange-coupled biradicals have found applications as polarizing agents in solid-state dynamic nuclear polarization (DNP),[1−6] building blocks in molecular magnetic materials,[7−13] polymerization initiators,[14−18] spin labels for structural investigation of biomolecules using interspin distance determination,[19−22] and molecular probes.[23−25] The magnitude and sign of the spin–spin coupling interaction (J) exert a crucial effect on the physiochemical properties of biradicals. The spin–spin coupling interaction can be through-bond and/or through-space,[26] and its value varies by many orders of magnitude.[10−12] Several factors, such as the nature of the linker between the two spins, the conformation, substituents, and the environment (e.g., temperature, solvent, etc.), control the magnitude of the exchange coupling in biradicals.[27] Through conformational constraints to enforce coplanarity of the two radical moieties with *m*-phenylene[10,28,29] or simple direct linkage,[30] stable trimethylenemethane (TMM)-type biradicals with large positive exchange interactions that show great potential as building blocks for robust magnetic materials have recently been obtained. In contrast, biradicals with rigid geometries that hold two nitroxide moieties approximately orthogonal to one another have weak exchange coupling but show enhanced DNP properties.[3−6] Therefore, a fundamental understanding of the factors controlling exchange coupling could allow the development of new biradicals with improved properties.

Most of the reported biradicals are based on two homogeneous radical parts rather than mixed radical moieties.[9] The latter case allows the combination of two different heterospin properties into unique molecules. It has recently been proposed[31−33] that mixed biradicals based on tetrathiatriarylmethyl (trityl) and nitroxide radicals are potentially the best biradical candidates to date for attaining the maximal DNP enhancement because of (1) the ideal electron paramagnetic resonance (EPR) frequency separation between the nitroxide g_{yy} component and the isotropic g value of trityl radicals and (2) their optimal relaxation times, which allow simultaneous microwave saturation and polarization turnover. The moderately weak coupling interaction in which J is typically smaller than the ^{14}N hyperfine splitting in the case of nitroxide biradicals[34] does not perturb the EPR frequency matching between the two spins and is a requisite for maximal enhancement. On the other hand, these trityl–nitroxide (TN) biradicals are well-suited for simultaneous measurement of oxygenation and redox status as well as thiol concentration

Received: November 26, 2012
Published: January 15, 2013

   dx.doi.org/10.1021/ja311571v | J. Am. Chem. Soc. 2013, 135, 2350−2356

by EPR spectroscopy and imaging, but the strong coupling interaction (typically, when J is >10 times the ^{14}N hyperfine splitting) is preferred in order to minimize the background signal.[35−37] Moreover, TN biradicals with strong ferromagnetic exchange coupling may have potential as building blocks for molecule-based magnetic materials.[7,13] Therefore, to expand the application of TN biradicals, there is a great need to be able to fine-tune the coupling interaction between the trityl and nitroxide moieties.

Our previous studies showed that the TN biradical TNN14 (Chart 1), which has a short, direct linkage between two radical moieties, has a large J value of 800 G at room temperature,[36] whereas TN1 and TSSN have much smaller J values of 300 and 100 G, respectively, because of the longer linker groups.[35,37] [It should be noted that in our previous and present studies, J denotes the triplet−singlet separation, its sign was not determined, and its units are presented in gauss (G), which can be converted into MHz through multiplication by 2.8.] These studies led us to the idea of fine-tuning the spin−spin coupling interaction in TN biradicals by varying the length of the linker group. In the present work, we synthesized the new TN biradicals CT02-GT, CT02-AT, CT02-VT, and CT02-PPT (Chart 1). While CT02-GT, CT02-AT, and CT02-VT have flexible linkers with various lengths between two radical parts, CT02-PPT has a rigid linker group. EPR spectroscopy coupled with computer simulation was used to investigate the temperature and linker-length dependence of the spin−spin coupling interactions in these new biradicals as well as in TN1 and TNN14. A survey of the EPR spectral profiles of TN biradicals with various coupling magnitudes in the range 0−1000 G was obtained using computer simulation. In addition, the **g**, hyperfine splitting, and the zero-field splitting tensors were determined from the solid-state EPR spectra.

Chart 1. Molecular Structures of the TN Biradicals

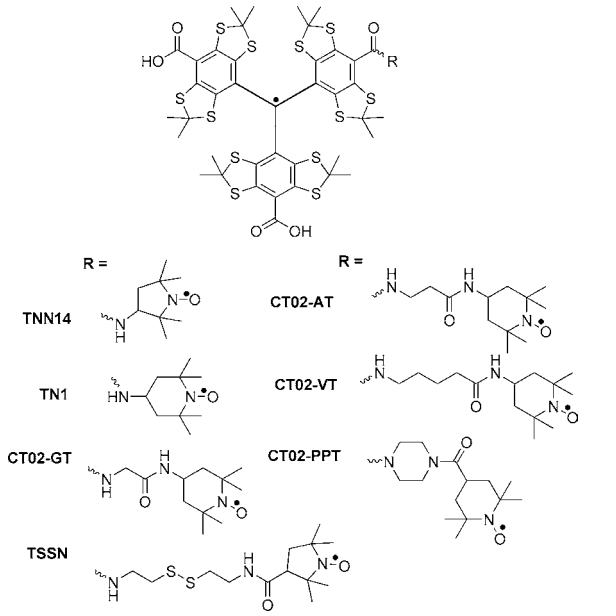

RESULTS AND DISCUSSION

Computer Simulations of EPR Spectra. Computer simulations of the EPR spectra in liquid and frozen solutions were carried out using the EPR simulation program (ROKI \EPR).[38] The fitting routine used to determine the J values of the TN biradicals was similar to the method described in our previous studies.[35−37] In the liquid state, the following parameters were optimized: g_1 and g_2; the hyperfine constant of the nitrogen atom, A_N; the relaxation or line-width variation parameters α, β, and γ; and J and its standard deviation ΔJ. The impact of the J distribution contributes to the line-width variation. All eight parameters (including ΔJ) were simultaneously optimized until the sum of the squares of the deviations between the experimental and calculated spectra was minimized. When the best J value was significantly larger than A_N, we checked the limit of J beyond which its further increase did not improve the fit significantly. The criterion was given by the noise of the experimental spectrum. We found that for the TN radicals, even when J exceeds A_N by an order of magnitude, the optimized value is still reliable. However, for the various nitroxide−nitroxide biradicals, reliable J values can be obtained only when J is a maximum of 3 times larger than A_N. Occasionally a superimposed signal of two conformers was observed. In this case, the two component spectra were described by the same parameters except for the J value, which was supposed to vary significantly with the molecular geometry.

Comparatively, the EPR spectral simulations in the solid state were more difficult since additional parameters such as the dipolar electron−electron interaction tensor (**D**), the anisotropic **g** tensors, and the hyperfine splitting tensors (**A**) had to be included. The Hamiltonian of a biradical can be written as

$$\hat{H} = J\hat{\mathbf{S}}_1\cdot\hat{\mathbf{S}}_2 + \hat{\mathbf{S}}_1\cdot\mathbf{D}\cdot\hat{\mathbf{S}}_2 + \hat{\mathbf{S}}_1\cdot\mathbf{g}_1\cdot\mathbf{B}\mu_B + \hat{\mathbf{S}}_2\cdot\mathbf{g}_2\cdot\mathbf{B}\mu_B + \hat{\mathbf{S}}_1\cdot\mathbf{A}_1\cdot\hat{\mathbf{I}}_1 + \hat{\mathbf{S}}_2\cdot\mathbf{A}_2\cdot\hat{\mathbf{I}}_2 \quad (1)$$

where $\hat{\mathbf{S}}$ and $\hat{\mathbf{I}}$ are electron and nuclear spin vector operators, **B** is the magnetic field vector, and μ_B is the Bohr magneton. We restricted the treatment to the case where the J coupling is stronger than the dipolar and hyperfine interactions and the Zeeman level separation for the two radical components. In this case, the $S = 1$ triplet state determines the EPR resonance and the $S = 1$ and $S = 0$ levels do not mix significantly. The effective $S = 1$ Hamiltonian can be written as

$$\hat{H} = \hat{\mathbf{S}}\cdot\mathbf{g}\cdot\mathbf{B}\mu_B + D\left[\hat{S}_z^{\,2} - \frac{1}{3}S(S+1)\right] + E(\hat{S}_y^{\,2} - \hat{S}_x^{\,2}) + \frac{1}{2}(\hat{\mathbf{I}}_1 + \hat{\mathbf{I}}_2)\cdot\mathbf{A}\cdot\hat{\mathbf{S}} \quad (2)$$

Here the components of the effective **g** tensor are given by $g_{ii} = (g_{1,ii} + g_{2,ii})/2$, where $i = x, y, z$. Similarly, the components of the effective hyperfine splitting tensor are also given by the arithmetical means $A_{ii} = (A_{1,ii} + A_{2,ii})/2$. The principal directions of the **g**, zero-field splitting, and hyperfine splitting tensors are supposed to be parallel. We still applied the above approach when the exchange coupling was comparable with the hyperfine interaction. This reduced the reliability of the optimized data, but the trend in the dipolar parameters characterizing the distance between the two unpaired electrons when different linkers were compared was still found to be correct.

The simulations required the optimization of three tensors with a total of eight elements (three for the **g** tensor, three for the **A** tensor, and two for the zero-field or dipolar tensor). Furthermore, the line width was also optimized. To obtain the best fit for the nine nonlinear parameters, a combination of various strategies was necessary. As a great number of local

dx.doi.org/10.1021/ja311571v | J. Am. Chem. Soc. 2013, 135, 2350−2356

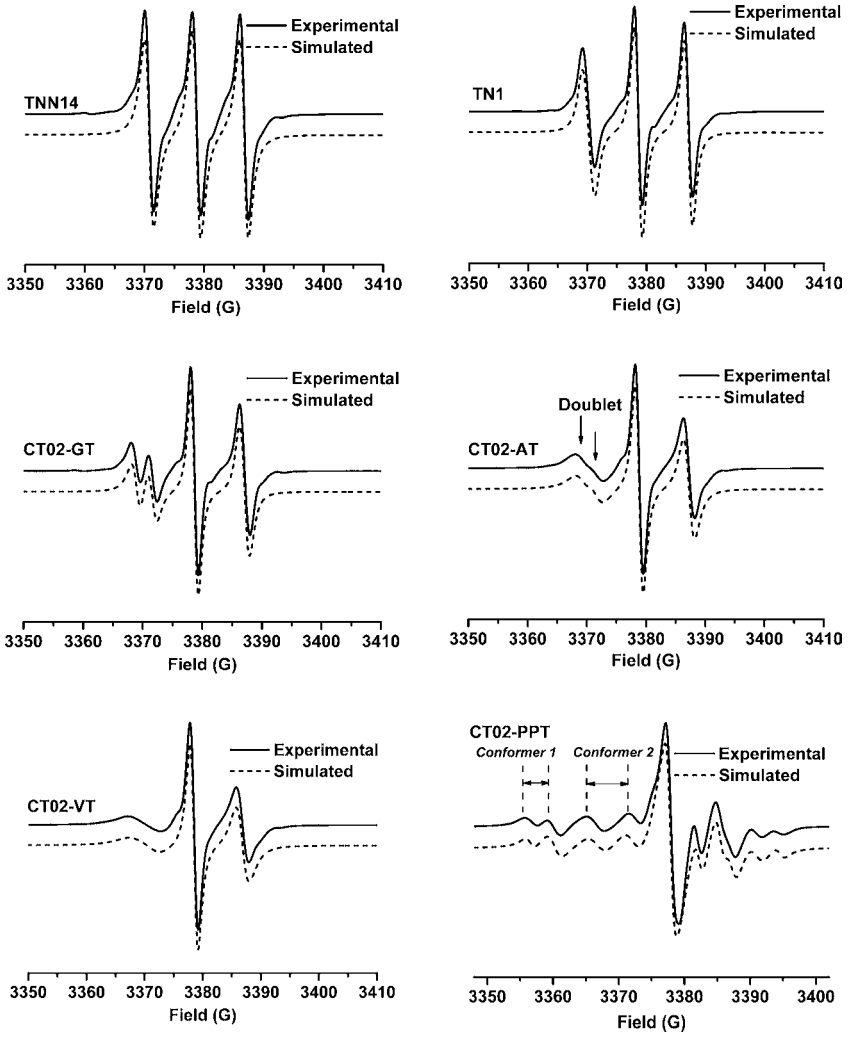

Figure 1. Experimental and simulated EPR spectra of TN biradicals at 357 K.

minima exist on the nine-dimensional error surface, the choice of the initial parameter set was very important. Typically around 100 different starting parameter sets were examined before automatic adjustment of the nine parameters offered the best available fit.

Experimental Studies of the Effect of Linker Distance on the Spin–Spin Coupling Interaction in TN Biradicals. Figure 1 shows the EPR spectra at 357 K for several TN biradicals, among which CT02-VT, CT02-AT, CT02-GT, and CT02-PPT were newly synthesized and TNN14 and TN1 were previously reported.[35,36] Because of variations in the magnitude of the spin–spin coupling interaction, these biradicals exhibit markedly different EPR spectral profiles. TNN14 and TN1 exhibited triplet EPR signals with J = 1230 and 430 G, respectively, which are higher than the reported values of ∼160 G for TN1 and ∼400 G for TNN14 at room temperature.[35,36] Because of the stronger spin–spin coupling interaction, TNN14 has a symmetric triplet signal, as opposed to the asymmetric signal with a relatively weak low-field peak observed for TN1. Despite the direct linkage between the two radical moieties through an amide bond, the use of the pyrrolidinyl nitroxide in TNN14 instead of the piperidinyl nitroxide in TN1 leads to a shorter distance between the two spins, and therefore, TNN14 exhibits a stronger spin–spin coupling interaction. The large J value for TNN14 indicates that the five-membered ring has an almost planar geometry that makes the C_2NO plane parallel to the central plane of the trityl moiety. In this case, the dominant spin–spin mechanism has through-bond character. While the biradicals CT02-GT, CT02-AT and CT02-VT have relatively flexible linkers with various lengths, CT02-PPT has a rigid linker. The longer linker in CT02-GT resulted in a significant decrease in the J value (J = 91 G) relative to TNN14 and TN1, as evidenced by the splitting of the low-field peak into a doublet (see the experimental EPR spectrum in Figure 1 and the calculated spectral pattern for J = 100 G in Figure 3). However, further increasing the linker length did not lead to a decrease in J. For instance, CT02-AT and CT02-VT have one and three more methylene groups between the two radical moieties than in CT02-GT, respectively, but they have similar J values (i.e., 91 G for CT02-GT, 110 G for CT02-AT, and 105 G for CT02-VT). For the latter two biradicals, the flexible linker led to a large scatter in the J values (ΔJ = 7.5 G for CT02-GT, 17 G for CT02-AT, and 20 G for CT02-VT) and broadened their low-field doublets into less-resolved patterns (Figure 1). Previously, a similar result was observed for TSSN, which has a J value of 82 G but affords an unresolved low-field doublet because of its long and flexible cystamine linker between nitroxide and trityl moieties.[37] The linker-length-independent J values for CT02-GT, CT02-AT, CT02-VT, and TSSN are most likely due to fast

dx.doi.org/10.1021/ja311571v | J. Am. Chem. Soc. 2013, 135, 2350–2356

folding of the flexible linkers, which leads to averaging of different conformations and produces geometries where the distances between the two radical centers are almost the same for the four biradicals. Therefore, the through-space spin−spin interactions are dominant for CT02-GT, CT02-AT, CT02-VT, and TSSN. A through-space exchange coupling interaction between the diagonal nitroxides was similarly observed in calix[4]arene nitroxide tetraradicals and diradicals.[26] Interestingly, CT02-PPT with the long but rigid linker afforded a complicated EPR spectrum with two separated doublets at low field, possibly due to the presence of two stable conformers (conformers 1 and 2) whose interconversion is relatively slow and whose characteristic EPR peaks are distinguishable even at the relatively high temperature (i.e., 357 K). Figure 2 shows the

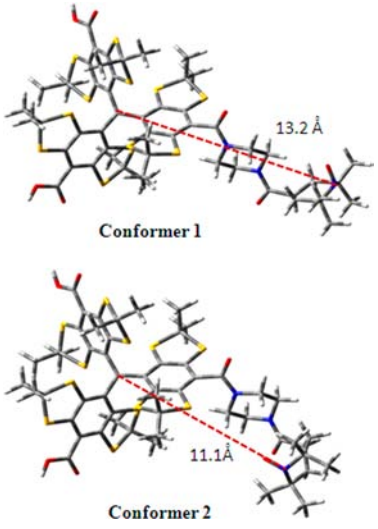

Figure 2. Two possible stable conformers of CT02-PPT showing different interspin distances. The structures were obtained on the basis of the most stable and unique conformers using Spartan '04 at the MMFF level.

structures of two possible stable conformers of CT02-PPT. Conformer 1 featuring the wing doublet pattern with a small J value of 3.7 G (Figure 1) has a relatively long interspin distance of 13.2 Å (Figure 2). In contrast, the inner doublet can be assigned to conformer 2 with an interspin distance of 11.1 Å, which affords an intermediate J value of 41 G.

Theoretical Investigation of the Effect of Spin−Spin Exchange Coupling on the EPR Spectra of TN Biradicals. Since fast molecular tumbling averages the anisotropic g, hyperfine, and dipolar interactions at a relatively high temperature (>293 K), only the spin−spin coupling interaction of TN biradicals exerts a significant effect on their EPR spectra, as shown above. Thus, computer calculations were carried out to describe the effect of the J value on the EPR spectra of TN biradicals quantitatively. Figure 3 shows simulated EPR spectra of TN biradicals as a function of J. When the trityl and nitroxide moieties are far away from each other and uncoupled (J = 0), the superimposed signals of the trityl radical (a single line, denoted by T) and the nitroxide radical (a triplet with a line separation of A_N = 17 G, denoted by N) can be observed. With an increase in J for $J < A_N$ (i.e., for J = 2 and 5 G), each line from the trityl and nitroxide signals splits into doublet, affording eight lines in total. When J is comparable to A_N (i.e., J = 10 and 25 G) forbidden transitions (*) appear along with the doublet lines. When J is moderately larger than A_N

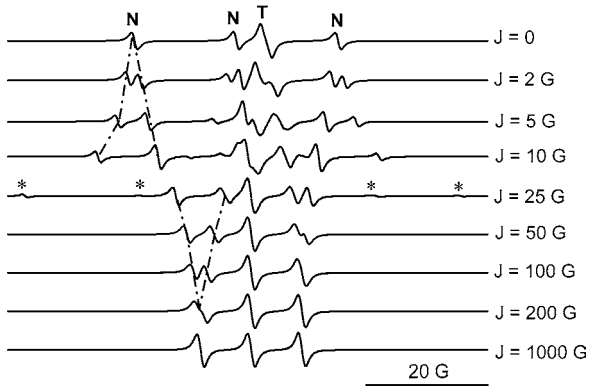

Figure 3. Simulated EPR spectra of TN biradicals with various J values. The simulation input standard deviation of J was set to ΔJ = zero, and no relaxation effect was considered. T and N indicate the trityl and nitroxide signals, respectively; forbidden transitions of biradicals are labeled with *.

(i.e., J = 25, 50, 100 G), a doublet pattern can be seen in the low-field region of the spectra. The separation of this doublet is inversely proportional to the J value. As J increases further, this doublet merges into singlet line (see the spectrum for J = 200 G), thus affording an EPR triplet pattern with a separation of approximately 8.5 G (A_N/2). When J is very large (i.e., J = 1000 G), the EPR spectrum is almost symmetric with the same width and amplitude for the triplet.

Temperature-Dependent Effect on J Coupling. As mentioned above, the predominant exchange mechanism has through-space character since the number of σ bonds in the linker does not play a decisive role in the magnitude of the spin−spin exchange coupling in the TN biradicals. Therefore, increasing the temperature could be expected to lead to different J values because of the possible variations of the interspin distance resulting from conformational changes.[26] As shown in Figure 4, for the TN biradicals with relatively short and rigid linkers (TNN14, TN1, and CT02-GT), J increased with temperature up to 357 K, which can be explained by the interconversion of two envelope or twist conformers of the five-membered nitroxide ring for TNN14 and two chair conformers of six-membered nitroxide ring for TN1 and CT02-GT. Their ground-state conformers correspond to the ring geometries with relatively longer distances between the nitroxide and trityl moieties, thus resulting in smaller J couplings. Because of the large J value for TNN14, the tendency of J to increase as a function of temperature was not that favorable. For CT02-AT and CT02-VT, J reached a maximal value at around 330−340 K. This behavior probably shows the activation of intramolecular rotation around the C_{sp^3}−C_{sp^3} bonds of the linker. The much higher J maxima for CT02-AT and CT02-VT relative to CT02-GT further verify that the spin−spin interaction of these TN biradicals has through-space character, whereas in TNN14 the interaction has through-bond character.

On the other hand, the substituted piperazine represents a rigid linker for which the exchange interaction between the radical centers is rather weak. In this case, the transition between the two chair conformers is slow, which allows for the detection of lines from the two conformers (i.e., conformers 1 and 2 of CT02-PPT in Figure 1). In conformer 2, which has a relatively large J value of 41 G at 357 K, the biradical adopts a geometry where the separation between the paramagnetic centers is relatively small. The increase in its J coupling with

dx.doi.org/10.1021/ja311571v | J. Am. Chem. Soc. 2013, 135, 2350−2356

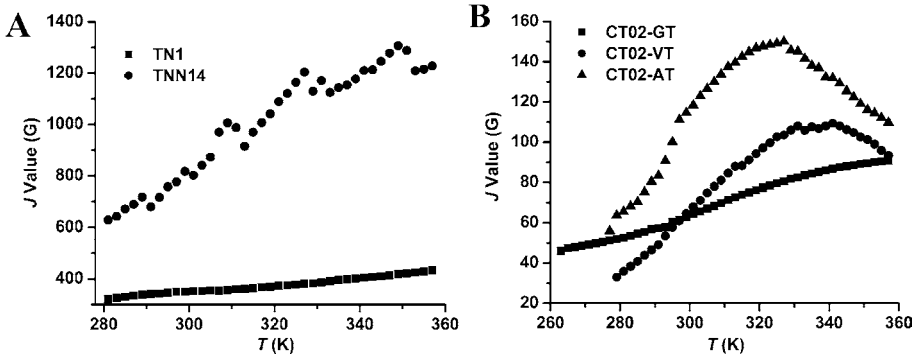

Figure 4. *J* values of TN biradicals (A) TN1 and TNN14 and (B) CT02-GT, CT02-AT, and CT02-GT as functions of temperature, obtained by simulating the corresponding EPR spectra at various temperatures.

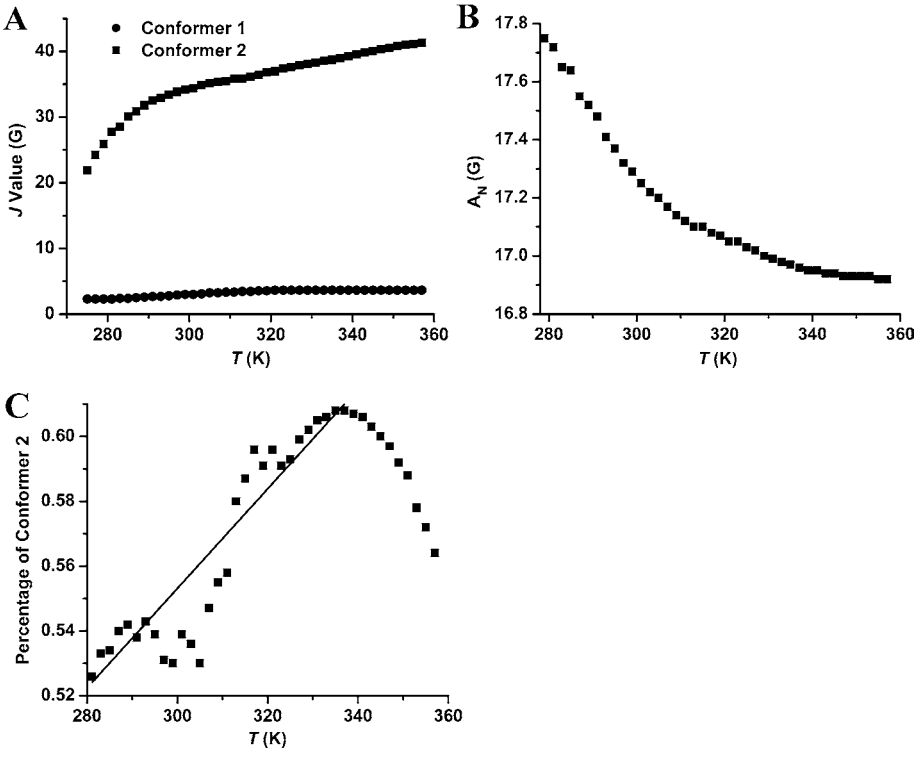

Figure 5. (A) *J* values of conformers 1 and 2, (B) hyperfine splitting (A_N), and (C) the population of conformer 2 of CT02-VT as functions of temperature, obtained by simulation of EPR spectra at various temperatures.

temperature can be attributed to the enhanced amplitude of oscillation of the ground-state chair conformation (Figure 5A). Since the oscillation can reduce the nonplanarity of the nitroxide moiety and accordingly decrease the A_N coupling, we examined the variation of A_N with temperature. As expected, A_N decreased from 17.75 G at 279 K to 16.92 G at 357 K (Figure 5B). Further inspection showed that the relative population of conformer 2 significantly increased with temperature, although it diminished at high temperature, indicating that conformer 1 has lower energy and is the ground-state conformer (Figure 5C).

Solid-State EPR Studies of TN Biradicals. The magnitude of the dipolar interaction and the anisotropic parameters for the **g** and hyperfine tensors are also important for the application of biradicals in structural studies. For this reason, estimation of these parameters from the frozen solution spectra was attempted. One critical step in this analysis is to compare the *J* exchange coupling with the hyperfine interaction. According to the EPR measurements in solution, the *J* exchange couplings of both TNN14 and TN1 are stronger than the dipolar and hyperfine interactions and the Zeeman level separation of the two radical components, and therefore, no significant triplet−singlet mixing can occur, that is, *J* is large enough to fulfill the restrictions of solid-state EPR simulation as mentioned above in the description of simulation program. Figure 6 shows the EPR spectra of TNN14 and TN1 at 220 K in a 1:1 (v/v) ethylene glycol/H_2O glass-forming solution, which can be analyzed well to give the tensor components for the *g*, hyperfine splitting, and zero-field splitting interactions. Since trityl radical is a stable carbon-centered radical with small spin−orbit coupling, a very small *g* anisotropy was observed in the solid state, with all of the *g* values being approximately 2.0030. In contrast, the g_{zz} value of the nitroxide radical is close to 2.0023 and its g_{xx} and g_{yy} values are typically 2.008−2.010 because of the significant spin−orbit coupling. While the *z* direction of the nitroxide monoradical is mainly determined by

dx.doi.org/10.1021/ja311571v | J. Am. Chem. Soc. 2013, 135, 2350−2356

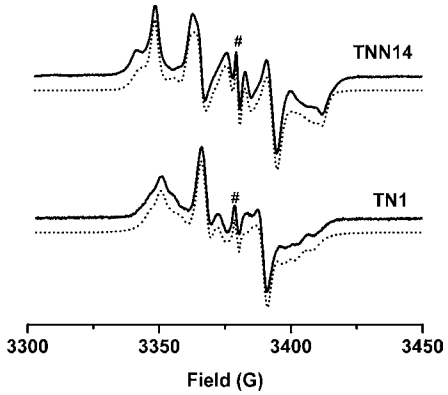

Figure 6. Experimental and simulated EPR spectra of TNN14 and TN1 at 220 K in a 1:1 (v/v) ethylene glycol/H_2O glass-forming solution. # denotes the signal of trityl monoradical.

the π lobe of the unpaired electron, the directions of the principal axes for the above biradicals are determined by the large zero-field (or dipolar) interaction. Since the g_{xx} values of the two biradicals (i.e., 2.0025 for TNN14 and 2.0028 for TN1) are nearly equal to the g_{zz} value of mononitroxide (2.0023), the x direction of the biradicals agrees with the direction of the π lobes of the nitroxide moiety where the unpaired electron is localized. The same assignment follows from the hyperfine splitting constant values (i.e., for trityl radicals $A_{xx} = A_{yy} = A_{zz} = 0$, while for nitroxides A_{zz} = 34−36 G, $A_{xx} = A_{yy}$ = 5−8 G), which are in excellent agreement with the values in Table 1. Since the rhombic zero-field parameter E is small, the z direction of the biradical is determined by the axis connecting the two radical centers. According to the point−dipole approach, the distance R between the radical centers can be found from the zero-field D term as $R = (27810/D)^{1/3}$. This relation gives R = 10.6 Å for TN1 and R = 9.7 Å for TNN14. The **g**, **D**, and **A** tensors of the two biradicals have nearly the same values at different temperatures, except for the different line widths.

For CT02-GT, the small g_{zz} value of 2.0028 (Table 1) and the large A_{zz} value of 18.5 (Table 1), which is close to half of a typical nitroxide radical A_{zz} (34−36 G), indicate that the lobe of the unpaired electron on the nitroxide moiety is parallel to the line connecting the two radical centers in this biradical. The very different **g** and hyperfine tensors for CT02-GT compared with the mononitroxides indicate that the J exchange coupling is indeed larger than the hyperfine interaction. In the case of CT02-AT, the A_{xx} value is very small (∼0 G, Table 1) perhaps because the J coupling has a value comparable to the hyperfine coupling, resulting in significant triplet−singlet mixing and uncertainty in the tensor components. Similar to CT02-GT, CT02-AT has an A_{zz} value close to half of the value for nitroxide monoradical, indicating that the direction of the π lobes of the nitroxide moiety is almost parallel to the line interconnecting the two radical centers.

As for CT02-VT, both the g and hyperfine values are typical for nitroxide monoradical, implying that the J exchange coupling is comparable to or less than the hyperfine coupling. Thus, the D value and the calculated value of the distance R between the radical centers are very approximate, and the same is also true for CT02-PPT. The negligible D values are in accordance with the extrapolated small J values at low temperature, since D and J should be on the same order of magnitude.

CONCLUSION

We have investigated the effects of the linker length and temperature on the spin−spin coupling interaction in TN biradicals. The coupling magnitude can be easily tuned from ∼4 to 1200 G by changing the nature and length of the tether group. Further tuning of the coupling interaction can be also achieved by varying the temperature. Depending on the coupling magnitude, these TN radicals could find various applications in redox sensing, magnetic materials, and DNP enhancement. The biradical CT02-PPT with a relatively small exchange interaction should be a good candidate as a DNP agent, and the DNP enhancement induced by TN biradicals could be further expanded by replacing the piperazine linker with a more rigid and bulky linker.[4−6] Overall, our present work provides a fundamental understanding of the spin−spin interaction in TN and other biradicals and could shed light on the design of new TN biradicals with desirable properties.

EXPERIMENTAL SECTION

Synthesis of the TEMPO Derivatives GT, AT, VT, and PPT. To a solution of Boc-glycine (201 mg, 1.15 mmol) in dry CH_2Cl_2 (25 mL) at 0 °C were added successively 4-amino-2,2,6,6-tetramethylpiperidine-*N*-oxyl (4-amino-TEMPO) (216 mg, 1.26 mmol), *N*,*N*-diisopropylethylamine (DIPEA) (300 μL), 1-hydroxybenzotriazole (HOBt) (80%, 213 mg, 1.26 mmol), and 1-(3-dimethylaminopropyl)-3-ethylcarbodiimide hydrochloride (EDCI) (265 mg, 1.38 mmol). The resulting orange solution was stirred at room temperature for 14 h and then washed with saturated aqueous NH_4Cl solution. The aqueous phase was separated and extracted once with CH_2Cl_2, and the combined organic layers were dried (Na_2SO_4), filtered, and concentrated in vacuo. Chromatography of the residue on SiO_2 (1−6% methanol in CH_2Cl_2) afforded 313 mg (83%) of GT as a red solid. HRMS (ESI) m/z: calcd for $C_{16}H_{30}N_3NaO_4^{\bullet+}$ ($[M + Na]^+$), 351.2134; found, 351.2151. The product was used in the next step without further characterization. A similar procedure was utilized for the syntheses of AT and VT, using Boc-β-alanine and 5-(Boc-amino)-valeric acid, respectively, as the starting material instead of Boc-glycine. In addition, PPT was synthesized from 4-carboxy-TEMPO and 1-Boc-

Table 1. Anisotropic Values of the Components of the g, Hyperfine Splitting (A_N), and Zero-Field Splitting (D) Tensors of the Biradicals

	g			A_N (G)			D (G)		
biradical	g_{xx}	g_{yy}	g_{zz}	A_{xx}	A_{yy}	A_{zz}	D_{xx}	D_{yy}	D_{zz}
TNN14	2.0025	2.0048	2.0057	18.0	3.9	2.8	−10.0	−10.4	20.4
TN1	2.0028	2.0040	2.0063	17.9	5.8	3.8	−7.8	−7.8	15.6
CT02-GT	2.0039	2.0070	2.0028	1.1	0	18.5	−3.3	−9.0	12.3
CT02-AT	2.0016	2.0088	2.0040	0	7.3	15.9	−3.0	−3.7	6.6
CT02-VT	2.0103	2.0057	2.0027	0	4.4	38	−1.9	−0.8	2.7
CT02-PPT	2.0046	2.0049	2.0027	0.5	1.0	40	1	−3	2

dx.doi.org/10.1021/ja311571v | J. Am. Chem. Soc. 2013, 135, 2350−2356

piperazine using a similar procedure. AT (250 mg, 86%): HRMS (ESI) m/z: calcd for $C_{17}H_{32}N_3NaO_4^{\bullet+}$ ([M + Na]$^+$), 365.2291; found, 365.2295. VT (230 mg, 78%): HRMS (ESI) m/z: calcd for $C_{19}H_{36}N_3NaO_4^{\bullet+}$ ([M + Na]$^+$), 393.2604; found, 393.2620. PPT (183 mg, 75%): HRMS (ESI) m/z: calcd for $C_{19}H_{34}N_3NaO_4^{\bullet+}$ ([M + Na]$^+$), 391.2447; found, 391.2442.

Synthesis of the TN Biradicals CT02-GT, CT02-AT, CT02-VT, and CT02-PPT. To a solution of GT (3.0 mg, 9.1 μmol) in dichloromethane (1 mL) was added trifluoroacetic acid (TFA) (1 mL). The reaction mixture was stirred for 3 h at room temperature and evaporated to dryness under vacuum. The residue was redissolved in 1 mL of *N*,*N*-dimethylformamide (DMF) and added dropwise to a solution of CT-03[39] (10 mg, 10 μmol), HOBt (80%, 4.6 mg, 27 μmol), (benzotriazol-1-yloxy)tris(dimethylamino)phosphonium hexafluorophosphate (BOP) (4.4 mg, 10 μmol), and DIPEA (15 μL) in dry DMF (4 mL). The resulting reaction mixture was continuously stirred for 18 h at room temperature, after which the solvent was removed under vacuum. The residue was dissolved in phosphate buffer (0.1 M, pH 7.4) and purified by column chromatography on reversed-phase C18 using water followed by 0–25% acetonitrile in water as eluents to give CT02-GT as a green solid (6.4 mg, 58%). HRMS (MALDI-TOF, DHB as the matrix) m/z: calcd for $C_{51}H_{59}N_3O_7S_{12}^{\bullet\bullet+}$ ([M]$^+$), 1209.100; found, 1209.049; calcd for $C_{51}H_{59}N_3NaO_7S_{12}^{\bullet\bullet+}$ ([M + Na]$^+$), 1232.089; found 1232.051.

A similar procedure was utilized for the syntheses of CT02-AT, CT02-VT, and CT02-PPT using AT, VT, and PPT as the starting materials, respectively. CT02-AT (5.4 mg, 60%): HRMS (MALDI-TOF, DHB as the matrix) m/z: calcd for $C_{52}H_{61}N_3O_7S_{12}^{\bullet\bullet+}$ ([M]$^+$), 1223.116; found, 1223.049; calcd for $C_{52}H_{61}N_3NaO_7S_{12}^{\bullet\bullet+}$ ([M + Na]$^+$), 1246.105; found, 1246.058. CT02-VT (4.1 mg, 52%): HRMS (MALDI-TOF, DHB as the matrix) m/z: calcd for $C_{54}H_{66}N_3O_7S_{12}^{\bullet\bullet+}$ ([M + H]$^+$), 1252.154; found, 1252.158; calcd for $C_{54}H_{65}N_3NaO_7S_{12}^{\bullet\bullet+}$ ([M + Na]$^+$), 1274.136; found, 1274.177. CT02-PPT (6.8 mg, 38%): HRMS (ESI) m/z: calcd for $C_{54}H_{63}N_3NaO_7S_{12}^{\bullet\bullet+}$, ([M + Na]$^+$), 1272.1212; found, 1272.1179.

■ ASSOCIATED CONTENT

Ⓢ Supporting Information

Spectroscopic characterization of new biradicals. This material is available free of charge via the Internet at http://pubs.acs.org.

■ AUTHOR INFORMATION

Corresponding Author

rocky@chemres.hu; Jay.Zweier@osumc.edu

Notes

The authors declare no competing financial interest.

■ ACKNOWLEDGMENTS

This work was supported by NIH Grants HL38324, EB0890, and EB4900 to J.L.Z. and HL81248 to F.A.V.

■ REFERENCES

(1) Song, C. S.; Hu, K. N.; Joo, C. G.; Swager, T. M.; Griffin, R. G. *J. Am. Chem. Soc.* **2006**, *128*, 11385–11390.

(2) Dane, E. L.; Maly, T.; Debelouchina, G. T.; Griffin, R. G.; Swager, T. M. *Org. Lett.* **2009**, *11*, 1871–1874.

(3) Dane, E. L.; Corzilius, B.; Rizzato, E.; Stocker, P.; Maly, T.; Smith, A. A.; Griffin, R. G.; Ouari, O.; Tordo, P.; Swager, T. M. *J. Org. Chem.* **2012**, *77*, 1789–1797.

(4) Zagdoun, A.; Casano, G.; Ouari, O.; Lapadula, G.; Rossini, A. J.; Lelli, M.; Baffert, M.; Gajan, D.; Veyre, L.; Maas, W. E.; Rosay, M.; Weber, R. T.; Thieuleux, C.; Coperet, C.; Lesage, A.; Tordo, P.; Emsley, L. *J. Am. Chem. Soc.* **2012**, *134*, 2284–2291.

(5) Kiesewetter, M. K.; Corzilius, B.; Smith, A. A.; Griffin, R. G.; Swager, T. M. *J. Am. Chem. Soc.* **2012**, *134*, 4537–4540.

(6) Matsuki, Y.; Maly, T.; Ouari, O.; Karoui, H.; Le Moigne, F.; Rizzato, E.; Lyubenova, S.; Herzfeld, J.; Prisner, T.; Tordo, P.; Griffin, R. G. *Angew. Chem., Int. Ed.* **2009**, *48*, 4996–5000.

(7) *Magnetism: Molecules to Materials*; Miller, J. S., Drillon, M., Eds.; Wiley-VCH: Weinheim, Germany, 2001–2003; Vols. *I–IV*.

(8) Iwamura, H.; Koga, N. *Acc. Chem. Res.* **1993**, *26*, 346–351.

(9) Rajca, A. *Chem. Rev.* **1994**, *94*, 871–893.

(10) Rajca, A.; Olankitwanit, A.; Rajca, S. *J. Am. Chem. Soc.* **2011**, *133*, 4750–4753.

(11) Shultz, D. A.; Fico, R. M.; Lee, H.; Kampf, J. W.; Kirschbaum, K.; Pinkerton, A. A.; Boyle, P. D. *J. Am. Chem. Soc.* **2003**, *125*, 15426–15432.

(12) Shultz, D. A.; Boal, A. K.; Farmer, G. T. *J. Am. Chem. Soc.* **1997**, *119*, 3846–3847.

(13) *Magnetic Properties of Organic Materials*; Lahti, P. M., Ed.; Marcel Dekker: New York, 1999.

(14) Yoshida, E.; Takeda, K. *Polym. J.* **2001**, *33*, 590–596.

(15) Bothe, M.; Schmidt-Naake, G. *Macromol. Chem. Phys.* **2004**, *205*, 208–216.

(16) Hill, N. L.; Braslau, R. *Macromolecules* **2005**, *38*, 9066–9074.

(17) Ruehl, J.; Hill, N. L.; Walter, E. D.; Milihauser, G.; Braslau, R. *Macromolecules* **2008**, *41*, 1972–1982.

(18) Kaim, A.; Pietrasik, K.; Stoklosa, T. *Eur. Polym. J.* **2010**, *46*, 519–527.

(19) Hubbell, W. L.; Cafiso, D. S.; Altenbach, C. *Nat. Struct. Biol.* **2000**, *7*, 735–739.

(20) Hagelueken, G.; Ingledew, W. J.; Huang, H.; Petrovic-Stojanovska, B.; Whitfield, C.; ElMkami, H.; Schiemann, O.; Naismith, J. H. *Angew. Chem., Int. Ed.* **2009**, *48*, 2904–2906.

(21) *Distance Measurements in Biological Systems by EPR*; Berliner, L. J., Eaton, G. R., Eaton, S. S., Eds.; Biological Magnetic Resonance, Vol. *19*; Kluwer: New York, 2000.

(22) Yang, Z. Y.; Liu, Y. P.; Borbat, P.; Zweier, J. L.; Freed, J. H.; Hubbell, W. L. *J. Am. Chem. Soc.* **2012**, *134*, 9950–9952.

(23) Marx, L.; Rassat, A. *Angew. Chem., Int. Ed.* **2000**, *39*, 4494–4496.

(24) Ishiguro, K.; Ozaki, M.; Sekine, N.; Sawaki, Y. *J. Am. Chem. Soc.* **1997**, *119*, 3625–3626.

(25) Roshchupkina, G. I.; Bobko, A. A.; Bratasz, A.; Reznikov, V. A.; Kuppusamy, P.; Khramtsov, V. V. *Free Radical Biol. Med.* **2008**, *45*, 312–320.

(26) Rajca, A.; Mukherjee, S.; Pink, M.; Rajca, S. *J. Am. Chem. Soc.* **2006**, *128*, 13497–13507.

(27) Forbes, M. D. E.; Dukes, K. E.; Avdievich, N. I.; Harbron, E. J.; DeSimone, J. M. *J. Phys. Chem. A* **2006**, *110*, 1767–1774.

(28) Rajca, A.; Takahashi, M.; Pink, M.; Spagnol, G.; Rajca, S. *J. Am. Chem. Soc.* **2007**, *129*, 10159–10170.

(29) Rajca, A.; Shiraishi, K.; Pink, M.; Rajca, S. *J. Am. Chem. Soc.* **2007**, *129*, 7232–7233.

(30) Suzuki, S.; Furui, T.; Kuratsu, M.; Kozaki, M.; Shiomi, D.; Sato, K.; Takui, T.; Okada, K. *J. Am. Chem. Soc.* **2010**, *132*, 15908–15910.

(31) Hu, K. N.; Bajaj, V. S.; Rosay, M.; Griffin, R. G. *J. Chem. Phys.* **2007**, *126*, No. 044512.

(32) Maly, T.; Debelouchina, G. T.; Bajaj, V. S.; Hu, K. N.; Joo, C. G.; Mak-Jurkauskas, M. L.; Sirigiri, J. R.; van der Wel, P. C. A.; Herzfeld, J.; Temkin, R. J.; Griffin, R. G. *J. Chem. Phys.* **2008**, *128*, No. 052211.

(33) Hu, K. N. *Solid State Nucl. Magn. Reson.* **2011**, *40*, 31–41.

(34) Hu, K. N.; Debelouchina, G. T.; Smith, A. A.; Griffin, R. G. *J. Chem. Phys.* **2011**, *134*, No. 125105.

(35) Liu, Y. P.; Villamena, F. A.; Rockenbauer, A.; Zweier, J. L. *Chem. Commun.* **2010**, *46*, 628–630.

(36) Liu, Y. P.; Villamena, F. A.; Song, Y. G.; Sun, J.; Rockenbauer, A.; Zweier, J. L. *J. Org. Chem.* **2010**, *75*, 7796–7802.

(37) Liu, Y. P.; Song, Y. G.; Rockenbauer, A.; Sun, J.; Hemann, C.; Villamena, F. A.; Zweier, J. L. *J. Org. Chem.* **2011**, *76*, 3853–3860.

(38) Rockenbauer, A.; Korecz, L. *Appl. Magn. Reson.* **1996**, *10*, 29–43.

(39) Liu, Y. P.; Villamena, F. A.; Sun, J.; Xu, Y.; Dhimitruka, I.; Zweier, J. L. *J. Org. Chem.* **2008**, *73*, 1490–1497.